Simulation-based inference (sbi) for pulsar population synthesis

Dr. Vanessa Graber (graber@ice.csic.es)

in collaboration with Michele Ronchi, Celsa Pardo Araujo, and Nanda Rea

SPINS-UK
November 2023

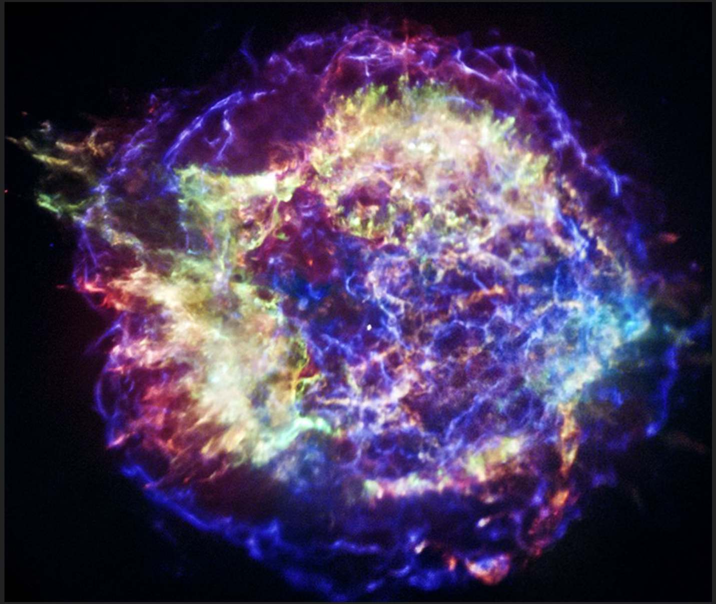

Cassiopeia A supernova remnant
(credit: NASA/CXC/SAO)

Population synthesis

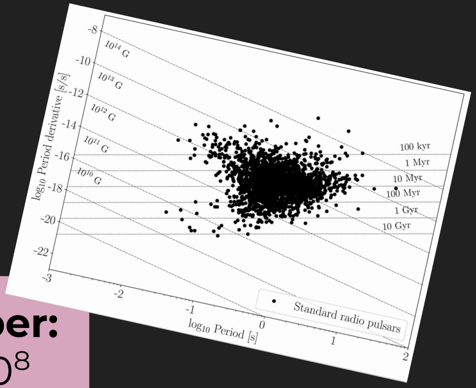

- We can estimate **the number of Galactic neutron stars**

CC supernova rate: ~ 2 per century × **Galaxy age:** ~ 13.6 billion years = **NS number:** ~ 2.8×10^8

- We only **detect** a very **small fraction** of all neutron stars. Population synthesis bridges this gap focusing on the full population of neutron stars (e.g. Faucher-Giguère & Kaspi 2006, Lorimer et al. 2006, Gullón et al. 2014, Cieślar et al. 2020):

model **birth properties** with Monte-Carlo approach → **evolve properties** forward in time → **apply filters** to mimic observational biases/limits → **compare** mock simulations **to observations** to constrain input

MAGNESIA erc CSIC Consejo Superior de Investigaciones Científicas IEEC

graber@ice.csic.es

Dynamical evolution

- **Neutron stars are born in star-forming regions**, i.e., in the Galactic disk along the Milky Way's spiral arms, **and receive kicks** during the supernova explosions.

- We make the following assumptions:
    - Electron-density model (Yao et al., 2017) + rigid rotation with T = 250 Myr.
    - **Exponential disk** with scale height h_c = 0.18 kpc (Wainscoat et al., 1992).
    - Single-component **Maxwell kick-velocity distribution** with dispersion σ_k = 265 km/s (Hobbs et al., 2005).
    - Galactic potential (Marchetti et al., 2019).

Artistic illustration of the Milky Way (credit: NASA JPL)

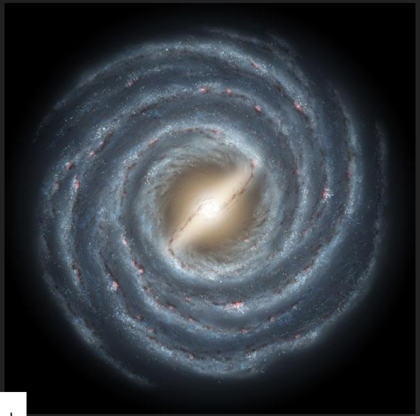

$$\mathcal{P}(z) = \frac{1}{h_c}\, e^{-\frac{|z|}{h_c}}$$

$$\mathcal{P}(v_\mathrm{k}) = \sqrt{\frac{2}{\pi}}\, \frac{v_\mathrm{k}^2}{\sigma_\mathrm{k}^3}\, e^{-\frac{v_\mathrm{k}^2}{2\sigma_\mathrm{k}^2}}$$

Solve Newtonian equations of motion to determine positions and velocities.

$$\ddot{\vec{r}} = -\vec{\nabla}\Phi_\mathrm{MW}$$

Dynamical evolution

- **Neutron stars are born in star-forming regions**, i.e., in the Galactic disk along the Milky Way's spiral arms, **and receive kicks** during the supernova explosions.

- We make the following assumptions:
    - Electron-density model (Yao et al., 2017) + rigid rotation with T = 250 Myr.
    - **Exponential disk** with scale height h_c = 0.18 kpc (Wainscoat et al., 1992).
    - Single-component **Maxwell kick-velocity distribution** with dispersion σ_k = 265 km/s (Hobbs et al., 2005).
    - Galactic potential (Marchetti et al., 2019).

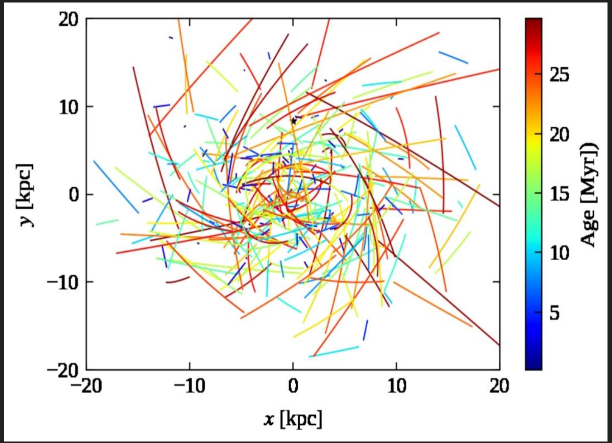

Top view of neutron-star evolution tracks in the Galaxy.

Solve Newtonian equations of motion to determine positions and velocities.

$$\ddot{\vec{r}} = -\vec{\nabla}\Phi_{\mathrm{MW}}$$

Magneto-rotational evolution I

- The neutron-star magnetosphere exerts a **torque onto the star**. This causes **spin-down** and **alignment of the magnetic and rotation axes**.
- Neutron star **magnetic fields decay** due to the Hall effect and Ohmic dissipation in the outer stellar layer (crust) (e.g., Viganó et al., 2013 & 2021).
- We make the following assumptions:
  - **Initial periods** follow a log-normal with μ_P and σ_P (Igoshev et al., 2022)
  - **Initial fields** follow a log-normal with μ_B and σ_B (Gullón et al., 2014)
  - Above $\tau \sim 10^6$ yr, **field decay** follows a power-law with $B(t) \sim B_0\,(1 + t/\tau)^{\alpha}$.

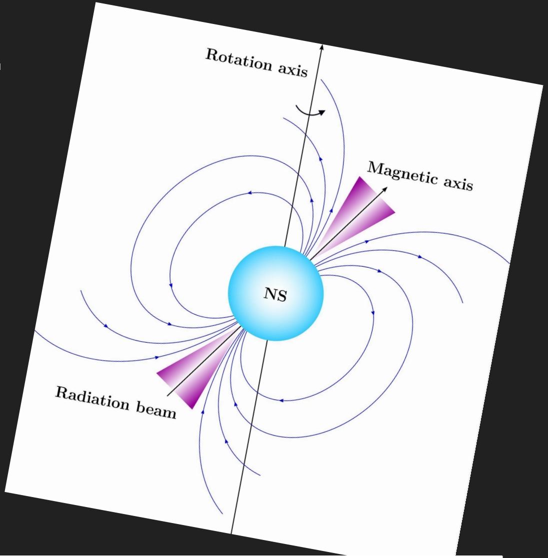

$$\mathcal{P}(\log P_0) = \frac{1}{\sqrt{2\pi}\sigma_P} \exp\left(-\frac{[\log P_0 - \mu_P]^2}{2\sigma_P^2}\right)$$

Here, we **vary** the five uncertain parameters **μ_P, μ_B, σ_P, σ_B** and **α**.

Magneto-rotational evolution II

- To model the magneto-rotational evolution, we numerically **solve two coupled ordinary differential equations** for the period and the misalignment angle (Aguilera et al., 2008; Philippov et al. 2014).

- We use results from **2D magneto-thermal simulations** to determine the evolution of the magnetic field.

- This allows us to follow the stars' P and $\dot{P}$ evolution in the $P\dot{P}$-plane.

Period period-derivative evolution tracks for $\mu_P = -0.6$, $\sigma_P = 0.3$, $\mu_B = 13.25$ and $\sigma_B = 0.75$.

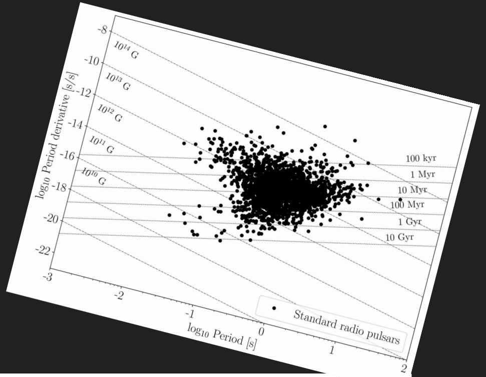

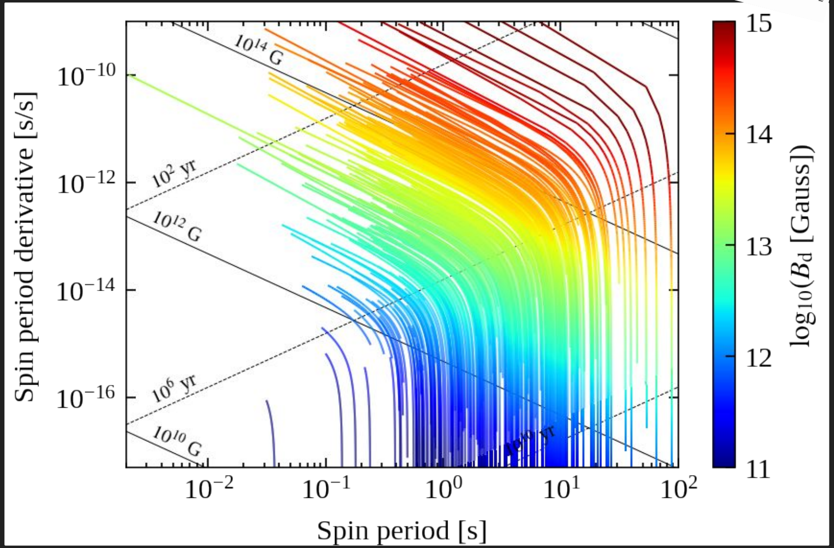

Detecting pulsars

- We model the **pulsar emission and beam geometry** to check if a pulsar is detectable.

- We then compare our mock populations with three surveys from Murriyang:
    - **Parkes Multibeam Pulsar Survey** (PMPS): *1,009 isolated pulsars*
    - **Swinburne Parkes Multibeam Pulsar Survey** (SMPS): *218 isol. p.*
    - **High Time Resolution Universe Survey** (HTRU): *1,023 isol. pulsars*

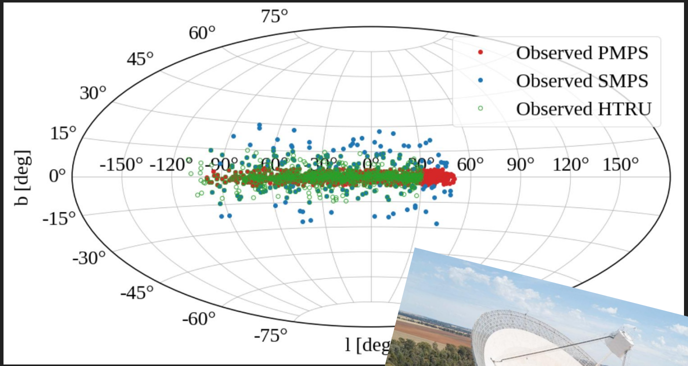

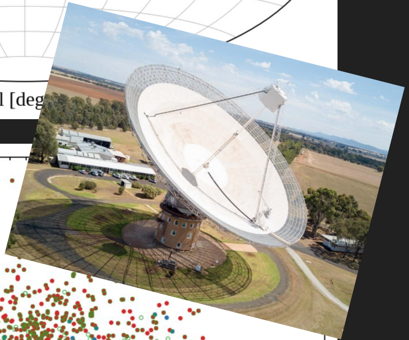

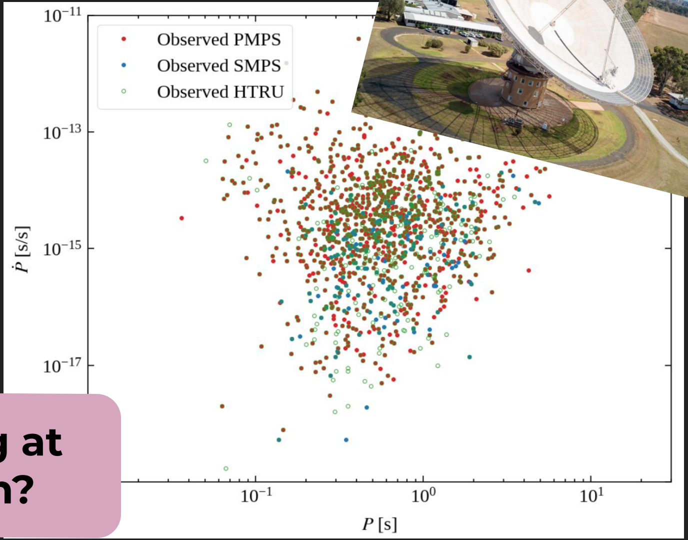

Can we constrain birth properties by looking at a current snapshot of the pulsar population?

Simulation-based inference (sbi)

- To perform **statistical inference for complex simulators where the likelihood is not known explicitly,** we use the following approach:

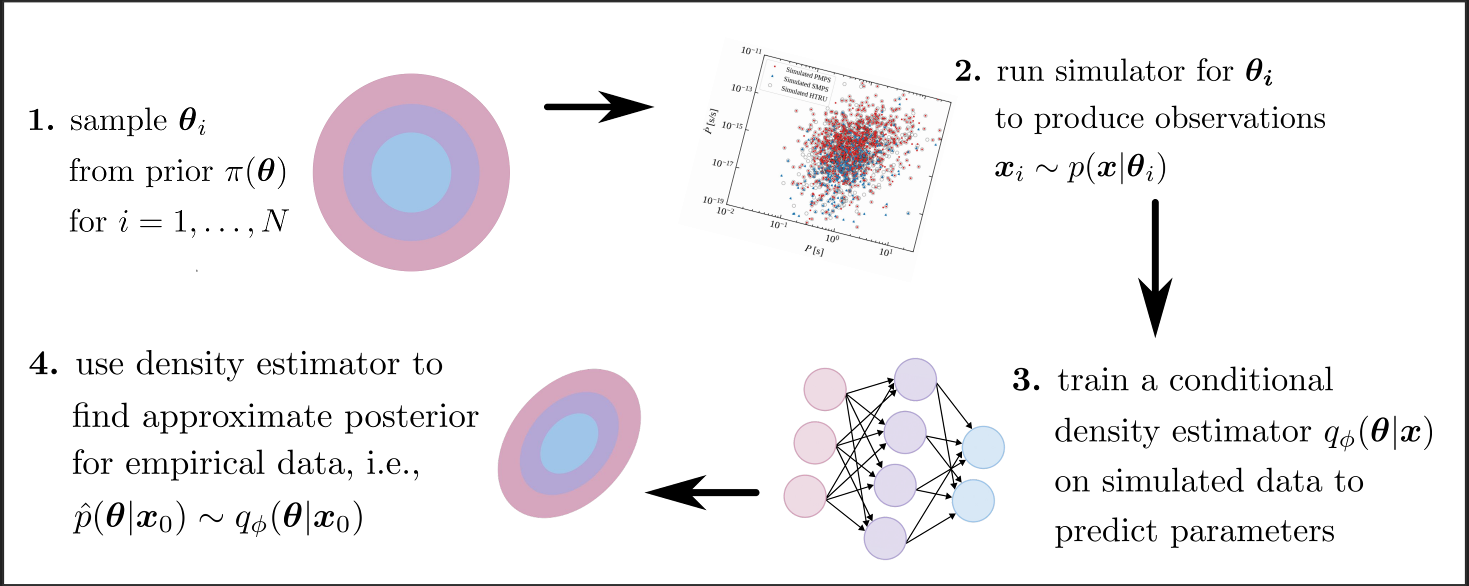

Workflow

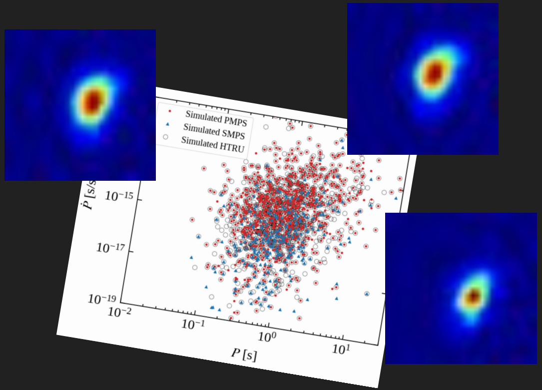

- We simulate **360,000 pulsar populations** varying μ_P, μ_B, σ_P, σ_B and α. We then **generate summary statistics**: 3 density maps for surveys in $P\dot{P}$-plane.

- To perform inference, we use **PyTorch-based toolbox sbi** (Tejero-Cantero et al., 2020; https://www.mackelab.org/sbi/). Our trainable neural network has two parts:
  - **CNN** (see Ronchi et al., 2021): compresses the data into a latent vector.
  - **Mixture density network**: approximate the posterior by a mixture of 10 Gaussians components; we learn the means, stds and coefficients.

The SBI algorithm we employ is based on Neural Posterior Estimation (NPE) (e.g., Papamakarios & Murray, 2016), **which allows us to directly learn the posterior.**

Posterior distributions for test sample

- As our conditional density estimator is represented by a neural network, we can **directly evaluate the posterior distributions for a given (test) observation**.

- We recover **narrow, well-defined posteriors** for all five parameters that typically contain the ground truth (parameters used for the forward simulation) at the 95% credibility level.

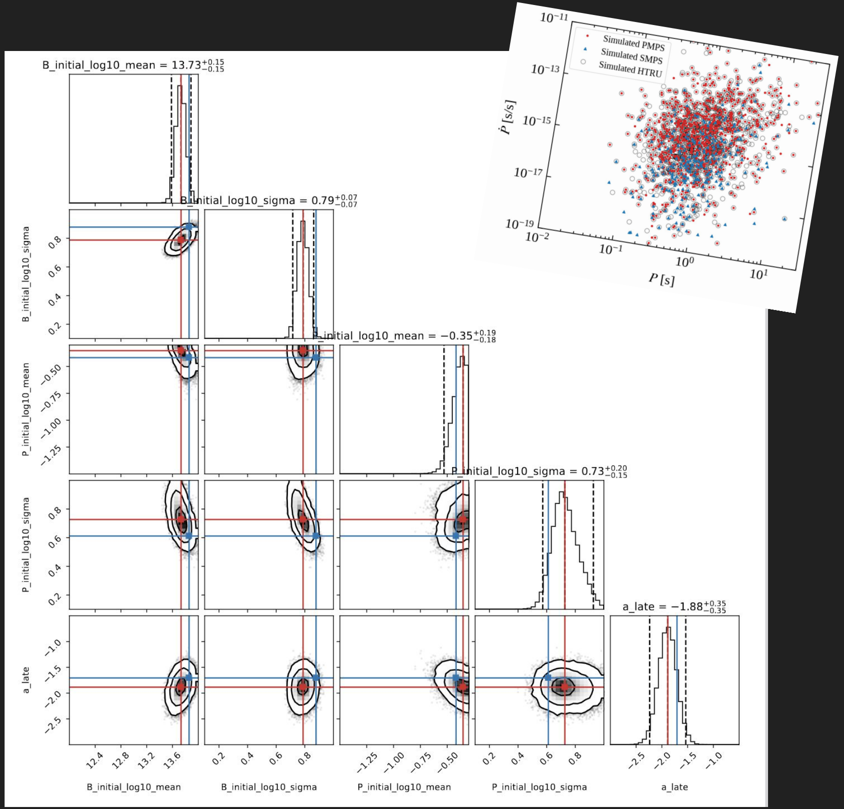

Posterior distributions for observed population

- With our optimised neural network, we can also **infer the posteriors** for the **pulsar population recorded in our three surveys** and recover the 95% credibility intervals:

$$\mu_B = 13.07^{+0.07}_{-0.08}$$

$$\sigma_B = 0.43^{+0.03}_{-0.03}$$

$$\mu_P = -0.98^{+0.25}_{-0.29}$$

$$\sigma_P = 0.54^{+0.33}_{-0.25}$$

$$\alpha = -1.77^{+0.35}_{-0.38}$$

$$\mathcal{P}(\log P_0) = \frac{1}{\sqrt{2\pi}\sigma_P} \exp\left(-\frac{[\log P_0 - \mu_P]^2}{2\sigma_P^2} \right)$$

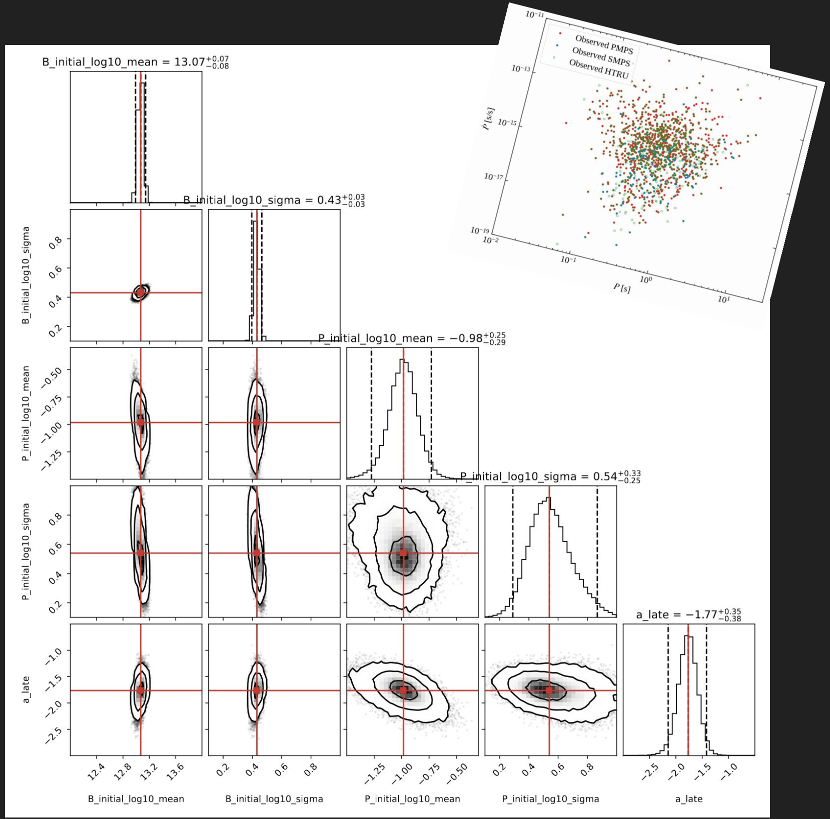

Robustness tests

- We **varied hyperparameters** of our DL approach to test the sensitivity of our inferred posteriors to those choices. We find similar training behaviour and optimisation losses and **robust results for magnetic-field and period inferences** but **larger variations for the late-time power-law index** α:

Test sample

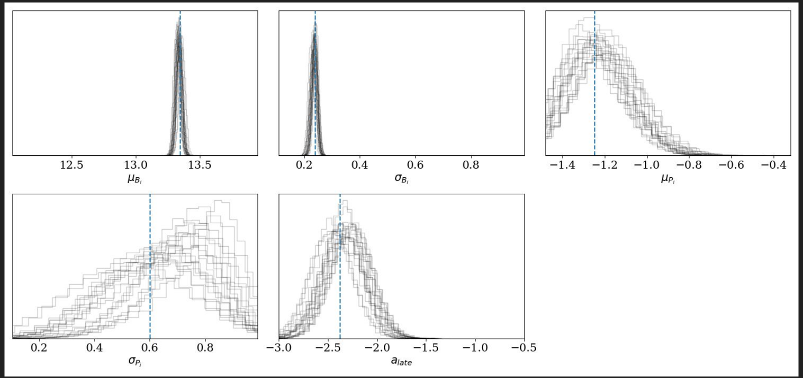

Observed sample

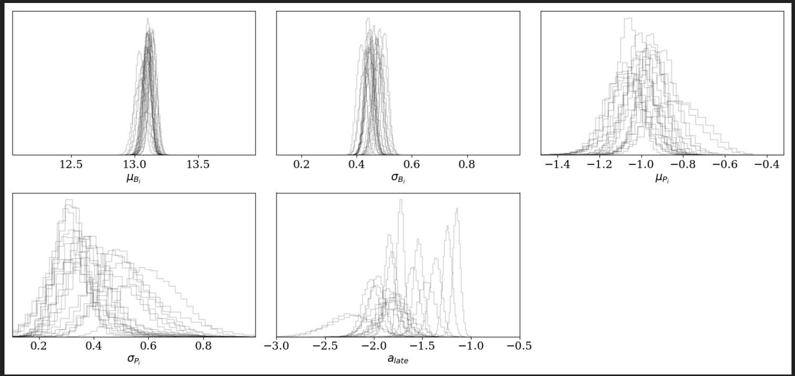

Robustness tests

- We **varied hyperparameters** of our DL approach to test the sensitivity of our inferred posteriors to those choices. We find similar training behaviour and optimisation losses and **robust results for magnetic-field and period inferences** but **larger variations for the late-time power-law index α**:

Test sample

Observed sample

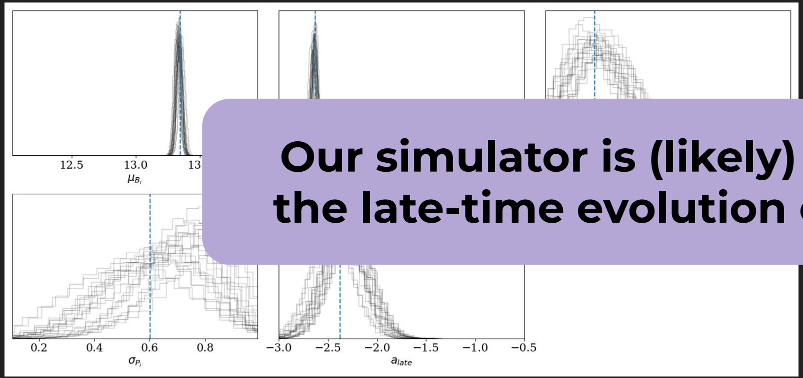

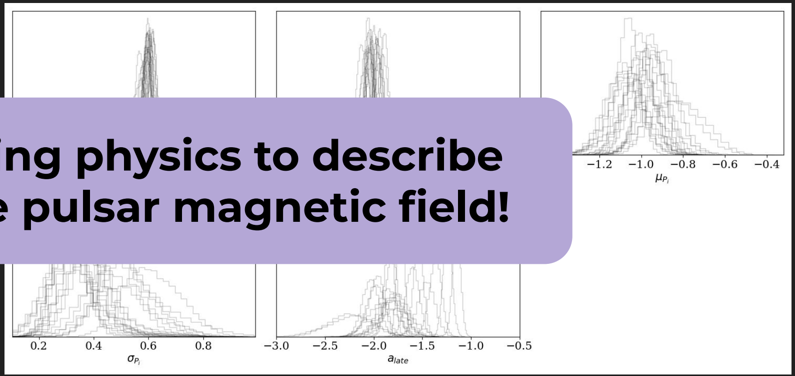

Our simulator is (likely) missing physics to describe the late-time evolution of the pulsar magnetic field!

THANK YOU

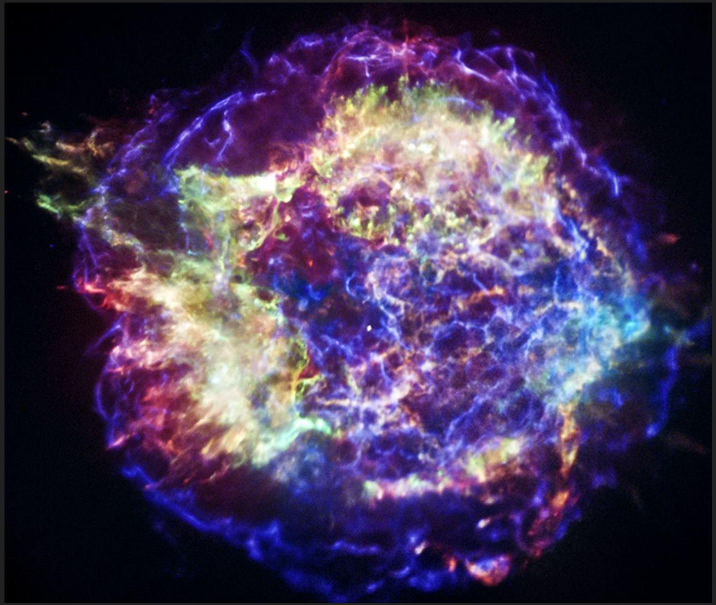

Cassiopeia A supernova remnant
(credit: NASA/CXC/SAO)

graber@ice.csic.es